Utah State University

From the SelectedWorks of Bela G. Fejer

January 1, 1986

The prereversal enhancement of thezonal electric field in the equatorial ionosphere

D. T. Farley
E. Bonelli
Bela G. Fejer, *Utah State University*
M. F. Larsen

Available at: https://works.bepress.com/bela_fejer/94/

JOURNAL OF GEOPHYSICAL RESEARCH, VOL. 91, NO. A12, PAGES 13,723–13,728, DECEMBER 1, 1986

The Prereversal Enhancement of the Zonal Electric Field in the Equatorial Ionosphere

D. T. FARLEY, E. BONELLI,[1] B. G. FEJER, AND M. F. LARSEN[2]

School of Electrical Engineering, Cornell University, Ithaca, New York

The electric fields in the ionospheric E and F regions near the magnetic equator often show a strong eastward enhancement shortly after sunset and before the eastward (normally) daytime field reverses to westward. Several theoretical models of the low-latitude fields suggest that this enhancement is caused mainly or entirely by F region winds (the F region dynamo), but some authors have suggested that it could be produced solely by E region tidal winds. We give here additional calculations and arguments in support of the F region source. The enhancement of the eastward field for an eastward F region wind turns out to be a simple direct consequence of the fact that after sunset the ionospheric conductivity decreases far more rapidly in the E region than in the F region.

INTRODUCTION

It is well known that the eastward daytime electric field in the E and F regions of the equatorial ionosphere often shows a significant and fairly sharp increase just before it reverses to its nighttime westward direction [e.g., *Balsley*, 1973; *Fejer et al.*, 1979; *Fejer*, 1981]. The E region changes are most easily seen in radar studies of the equatorial electrojet, while the F region fields can be observed via the motion of the F layer in ionograms and/or incoherent scatter measurements of the vertical plasma drift velocity. The magnitude of this prereversal enhancement depends upon various factors such as season, level of magnetic activity, and phase of the solar cycle. On a given day it might be absent, but it is a persistent feature of averaged data. Such electric field perturbations are generally not observed at the time of the sunrise reversal.

A number of numerical models of the global or equatorial dynamo electric fields and currents have been developed [e.g., *Heelis et al.*, 1974; *Matuura*, 1974; *Richmond et al.*, 1976; *Walton and Bowhill*, 1979; *Stening*, 1981; *Takeda and Maeda*, 1983], and some of these do show a sunset enhancement that agrees to some extent with the observations. However, none of these papers gives a very satisfying discussion of the physics of the enhancement; it is just a feature of the more successful models. For example, *Heelis et al.* [1974] simply point out that it is associated with the F layer dynamo, which was first discussed by *Rishbeth* [1971]. *Matuura* [1974] also concludes that the F region dynamo plays an important role in the prereversal enhancement. This dynamo, driven by F region winds, produces polarization fields and currents perpendicular to and parallel to the magnetic field. The latter provide a coupling to the E region and are of course affected by the sudden change in the E region conductivities at sunset. A fairly recent discussion of the F layer dynamo is given by *Rishbeth* [1981], where the question of the prereversal enhancement is mentioned but not dealt with in any detail.

Stening [1981] considers F region effects and shows a sketch illustrating some aspects of the sunset time current flow for one of his models, a (1, −2) diurnal tidal mode wind blowing only in the F region. The magnitude of Stening's enhancement is quite small, however, and is sensitive to the phase of his assumed wind pattern. *Takeda and Maeda* [1983] discuss the evening F region dynamo but not how it affects the prereversal enhancement. The model of *Richmond et al.* [1976] does not show the enhancement, presumably because it is driven only by E region winds. On the other hand, the calculations of *Walton and Bowhill* [1979], which also completely neglect the F region dynamo, do show some prereversal enhancement effects. Their calculations do include conjugate point coupling via field-aligned currents (symmetry between the hemispheres is not assumed), and they also consider the effects of differences in the geographic and dip equators, a difference that is particularly large at the longitude of the Jicamarca Radio Observatory. They argue that the F region dynamo is probably not needed to explain the prereversal enhancement, at least at Jicamarca.

In Figure 1 we show as examples three particular model curves, together with averaged (over altitude and for equinoxes during the two most recent solar maxima) F region vertical drift data from Jicamarca. The *Stening* [1981] curve is one of several models given in the paper and is from his Figure 8; similarly, the *Richmond et al.* [1976] curve is from their Figure 6, using the (1, −2) diurnal tide mode wind of *Tarpley* [1970]. An upward drift of 40 m/s corresponds to an eastward electric field of 1 mV/m. The enhancement is an obvious feature of the Jicamarca data and two of the model curves. Figure 2, adapted from *Balsley and Woodman* [1969], shows a particular example of a prereversal enhancement. The dashed part of the F region curve indicates some contamination by spread F echoes, the circles in the E region curve represent a lower limit of the drift velocity, and the horizontal dashed line is an estimate of the ion-acoustic velocity above which the E region drift velocity estimate becomes less and less accurate. It is important to note that the enhancement in this case is very abrupt, and it is observed simultaneously in both the equatorial E layer (electrojet data) and F layer, even though these regions are not directly coupled by magnetic field lines.

We have been developing a model of the equatorial fields ourselves, more or less along the lines followed by *Heelis et al.* [1974]. The full details of the model are given by *Bonelli*

[1] Presently at Departamento de Fisica, Universidade Federal do Rio Grande do Norte, Natal, Brazil.

[2] Presently at Department of Physics and Astronomy, Clemson University, Clemson, South Carolina.

Copyright 1986 by the American Geophysical Union.

Paper number 6A8603.
0148-0227/86/006A-8603$02.00

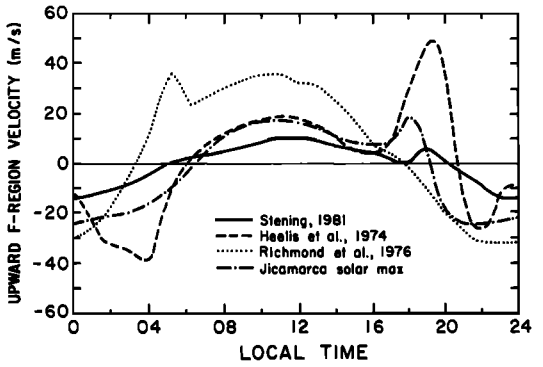

Fig. 1. Three models of the vertical plasma drift velocity in the equatorial F region compared with averaged Jicamarca data.

[1985]; the relatively modest goal here is to focus on the prereversal enhancement and its physical explanation, which turns out to be quite insensitive to moderate variations in many of the model parameters. All that is needed to produce the prereversal enhancement is a wind blowing eastward in the F region at the time of E region sunset.

Model

The ionosphere is represented by a thin E layer and a reasonably realistic extended F layer, with E and F region winds as the driving terms. The two regions are coupled by currents flowing along magnetic field lines into and out of the E region and by the mapping of electric fields along the assumed equipotential magnetic field lines. Beginning with the E region, say, we assume some initial distribution of current input from the F region and add the effect of the E region tidal winds. Using vertically integrated conductivities and the fact that div $\mathbf{J} = 0$, one can solve numerically for the electrostatic potential distribution in the E region; this potential is then mapped into the F region to give both the horizontal and vertical plasma drift velocities there. The vertical drift may or may not be used to modify the F region electron density profile for the next time (longitude) step. The horizontal drift velocity is always used, however, and is combined with the neutral F region model (density, temperature, and pressure) of *Jacchia* [1977] to give the F region neutral wind $\mathbf{U}$ (affected by ion drag) and currents perpendicular to $\mathbf{B}$, driven by the electric field mapped up from the E region and $\mathbf{U} \times \mathbf{B}$. Finally, setting div $\mathbf{J} = 0$ in the F region and integrating along the field lines gives the parallel current flowing into the E region, one of the inputs with which we began, and so the loop is closed. The whole calculation is then iterated until it converges. One can just as easily begin the calculation in the F region; the final result is the same.

For our simple two-dimensional E region model we follow *Heelis et al.* [1974] and assume that the integrated parallel, Pedersen, and Hall conductivities are proportional to the maximum electron density N_mE multiplied by 1.2×10^{-7}, 1.2×10^{-10}, and 2.0×10^{-10}, respectively in the MKS units. For some calculations, though, the Pedersen coefficient was doubled. For the daytime densities we assume

$$N_mE = 1.4 \times 10^{11}[(1 + 0.008\,R_z)\cos\chi]^{1/2}\ \mathrm{m}^{-3} \quad (1)$$

where R_z is the sunspot number and χ is the solar zenith angle. The nighttime N_mE is taken to be constant and equal to $5 \times 10^9\ \mathrm{m}^{-3}$. The E layer is assumed to be centered at 120 km. For the E region wind we follow *Tarpley* [1970] and others in choosing the symmetrical evanescent (1, −2) solar diurnal mode (or the (1, −1) mode in Tarpley's notation) in which the southward (u) and eastward (v) winds are taken to be proportional to sin $(\phi+\phi_0)$ and sin $(\phi+\phi_0+90°)$, respectively, where ϕ is longitude and $\phi = 0$ corresponds to the midnight meridian. The latitude dependence is given by rather complicated Hough function expressions, normalized so that the maximum value of both components is 130 m/s, again following *Tarpley* [1970]. The Hough function for u is negative in the northern hemisphere and positive in the southern. The value of ϕ_0 is typically somewhere near 270°, implying that the low-latitude poleward and eastward winds maximize near noon and 0600 LT, respectively.

The F region is assumed to be a simple Chapman layer, with values of N_{max} and scale height that can depend on longitude and solar activity but not latitude; h_{max} may or may not be allowed to change in accordance with the calculated vertical plasma drift velocity. The F region neutral atmosphere follows *Jacchia* [1977], and the F region winds are driven by pressure gradients (in the longitudinal direction only). As is mentioned above, ion drag effects are included self-consistently, taking into account the zonal ion drift velocity.

The calculations are made using an E region grid spacing of 1° in latitude and 5° in longitude, and the E region potential is assumed to be constant at 85° latitude and of course periodic in longitude. The high-latitude boundary conditions do not affect the low-latitude results significantly. Further discussion of the model is given by *Bonelli* [1985]; for the results to be presented here the details are not crucial. The calculations that are particularly relevant to the prereversal enhancement phenomenon were all done for equinox periods (symmetric hemispheres) with high solar activity. The magnetic field was approximated by a dipole aligned with the earth's axis of rotation.

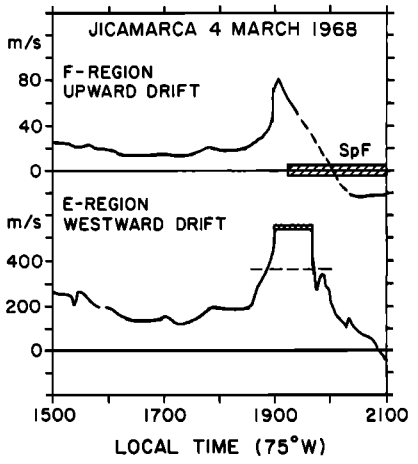

Fig. 2. A particular example of a prereversal enhancement at Jicamarca. The E region westward electron drift velocity and the F region upward plasma velocity are both proportional to the eastward electric field. Note that both increase sharply and simultaneously. The F region velocities are derived from incoherent scatter observations and the E region values from coherent radar echoes from the electrojet. Further explanation is given in the text (Adapted from *Balsley and Woodman* [1969]).

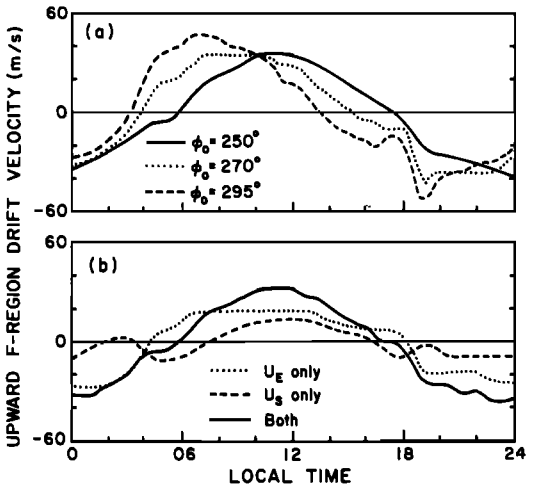

Fig. 3. Effect of (*a*) the phase ϕ_0 of the (1, −2) *E* region tidal wind on the vertical equatorial plasma drift at 300 km and (*b*) the southward (U_S) and eastward (U_E) winds for $\phi_0 = 250°$. *F* region dynamo effects are ignored here (no field-aligned currents).

A Few Results

E Region Dynamo Only

We first assume that the only driving term is the *E* region tidal wind described above. No currents are allowed to flow between the *E* and *F* regions, and so the electrostatic potential in both layers is determined by this tide. The results of the calculation are shown in Figure 3, in which Figure 3*a* illustrates the effect of a change in phase of the mode and Figure 3*b* shows separately the effects of the zonal and meridional wind components for the phase ($\phi_0 = 250°$) which best fits the observations. The parameter plotted is the vertical *F* region drift velocity (+40 m/s implies an eastward electric field of 1 mV/m).

Figure 3*a* shows some sign of an upward perturbation for the two larger phase angles, but these are postreversal, not prereversal effects, and the reversal times are much too early. Figure 3*b* makes clear the point that the north-south and east-west wind components are approximately equally important; the zonal wind for this phase produces a hint of the prereversal enhancement, but this perturbation is almost exactly cancelled by the contribution of the north-south wind. These results, as well as most of those of other modelers, strongly suggest that the effect we are interested in cannot in all likelihood be produced by plausible *E* region winds. Certainly, the sharp prereversal enhancement shown in Figure 2 cannot.

Uniform F Region Wind Only

In order to investigate in the simplest possible way the effect of the *F* region dynamo upon the electric fields, we assumed for this calculation that the only driving force was a uniform wind in the *F* region blowing from west to east with a velocity of 200 m/s at all latitudes and longitudes, i.e., independent of ion drag, and that h_{max} was kept fixed at 350 km, an altitude which maps down along the magnetic field lines to the *E* region at about 10° latitude. We also doubled the Pedersen conductivity coefficient to 2.4×10^{-10}, but these exact values are not important; moderate changes do not alter the qualitative picture. Some of the resulting equatorial drift velocities, which are equivalent to electric fields, are plotted in Figure 4. The top panel (Figure 4*a*) is the eastward ion drift near the peak of the *F* region; the middle panel (Figure 4*b*) is the vertical *F* region ion drift; and Figure 4*c* shows the westward *E* region electron drift velocity. The effect of sunset at 1800 LT is obvious; there is also a similar sunrise effect, but this simple model is not at all realistic then, and such sunrise enhancements are seldom seen in the data.

The top curve is easily explained. During the day the high impedance *F* region dynamo is shorted out by the highly conducting *E* region, and so the electric fields are nearly zero, and there is very little *F* region motion. Near sunset the *E* region electron density and conductivity drop rapidly to their constant nighttime values, but the *F* region density drops only slowly. The dynamo fields are then only partially shorted, and the eastward *F* region drift velocity reaches, in this example, a maximum value of about half the neutral wind velocity. (If the *E* region conductivity were small enough, the *F* region plasma would drift at exactly the wind velocity.) As the night progresses, the *F* region density continues to drop slowly, while the *E* region density stays constant (in our model, at least), and so the *F* region dynamo gradually becomes less and less effective.

Figures 4*b* and 4*c* show exactly the prereversal enhancement effects in the *E* and *F* regions that we are looking for. So it appears that all that is needed to produce these electric field enhancements is an eastward *F* region wind blowing at the time of *E* region sunset. With such a strong hint it should be possible to explain the phenomena using only simple physical arguments. This explanation is not entirely obvious, however, and is the main point of this paper, and so we postpone this discussion for the moment.

Figures 5 and 6 give us some additional information about the low-latitude region during the sunset and evening periods. Figure 5 gives the electrostatic potential at the top of the (two-dimensional) *E* region and is really just a slight extension of the information given in Figure 4, displayed in a different way. The electric field at the equator is eastward after sunset, reaches a maximum, and then declines, reversing shortly before 2000 LT. After reaching a mild westward maximum it declines again slowly. This is of course com-

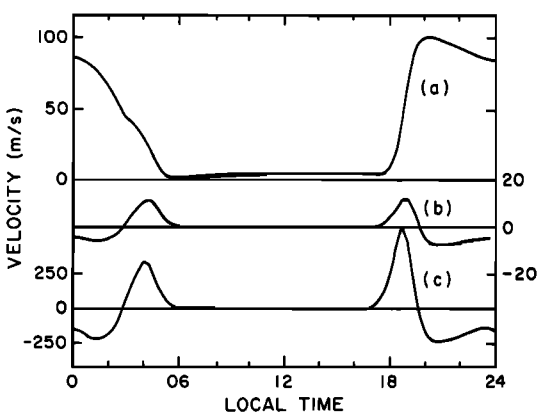

Fig. 4. Equatorial drift velocities driven by a uniform 200 m/s eastward *F* region dynamo wind only: (*a*) the eastward *F* region ion velocity at 350 km; (*b*) the upward *F* region ion velocity; and (*c*) the westward *E* region electron velocity. The *E* region drift velocity corresponds to an altitude of about 105 km and to a ratio of Hall to Pedersen electric field of 25. The sunset prereversal enhancements are clearly shown in Figures 4*b* and 4*c*. The model is not realistic near sunrise.

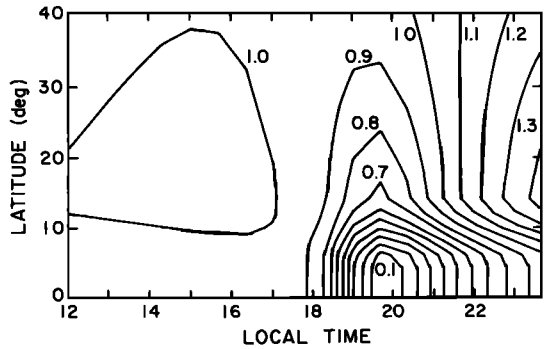

Fig. 5. Part of the electrostatic potential distribution in the E region for the uniform 200 m/s F region dynamo wind example. The contours are labeled in kilovolts.

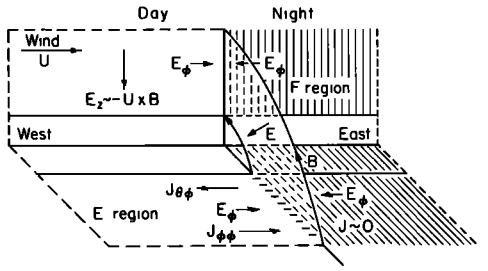

Fig. 7. Oversimplified model of the F region prereversal enhancement driven by a uniform F region wind U. Near the sunset terminator the F region dynamo E_z is no longer shorted out and approaches $-\mathbf{U} \times \mathbf{B}$. This field maps to an equatorward E_θ (not shown explicitly) in the E layer and drives a westward Hall current. But if no current flows in the nightside E region, a negative polarization charge must develop at the terminator, with E_ϕ as is shown and $J_{\phi\phi}$ cancelling $J_{\phi\theta}$, and this E_ϕ maps back to the F region and causes first an upward, then a downward, $\mathbf{E} \times \mathbf{B}$ plasma drift.

pletely consistent with the E region electron drift in Figure 4*c*, as it must be. The F region fields near h_{max} map down along the magnetic field to the E region at about 10° latitude, where the meridional field is always southward (i.e., equatorward), giving a downward field and eastward drift in the F region. The zonal field is first eastward, then westward, reversing somewhat before 2000 LT. All of this behavior is consistent with Figures 4*a* and 4*b*. A final point worth noting, although it is quite difficult to see in Figure 5, is that there is a very slight poleward component of the electric field just off the equator.

Figure 6 is important for our understanding of Figures 4 and 5. We have plotted the current density flowing out of the E region parallel to the magnetic field and into the F region, for the latitudes and times of most interest. Positive currents are upward and equatorward. By symmetry the current is zero at the equator. The key feature to note here is the strong upward maximum at about 6° latitude and the reversal to downward at about 9°. Multiplying this curve by the sine of the dip angle to get the upward component of $J_\parallel$ does not change these basic features.

INTERPRETATION

The behavior of the vertical electrical field and the eastward drifts in the F region for the pure F region dynamo calculation has already been discussed and is quite easy to understand. The wind U tries to drive the field to a value of $-\mathbf{U} \times \mathbf{B}$ but is prevented from doing so to some degree by the E region, depending upon the relative magnitudes of the integrated E and F region Pedersen conductivities. The

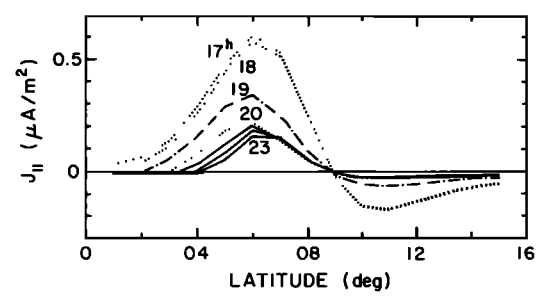

Fig. 6. Late afternoon and evening currents flowing out of the low-latitude E region, parallel to the magnetic field, and into the F region, for the uniform F region dynamo wind example. Positive currents are upward and equatorward.

considerably more difficult question is just how this vertical F region electric field generates the observed zonal F region and electrojet fields. The generation occurs in the E region, where the field-aligned coupling currents must close in a divergence-free manner, but the details turn out to be more complicated than one might suspect.

We can understand part of the process by considering the very oversimplified model, sketched in Figure 7. The dayside of the figure is taken to be near sunset, with the F region dynamo reasonably effective, so that E_z is some significant fraction of $-\mathbf{U} \times \mathbf{B}$. This field maps to an equatorward meridional E region field E_θ (not shown explicitly, to avoid cluttering the figure), which tries to drive a westward (i.e., opposite to the normal daytime E region dynamo current) zonal current $J_{\phi\theta}$ (J is the vertically integrated horizontal current density; θ and ϕ are polar coordinates). But if we assume that the E region electron density drops suddenly to a very low value at sunset, only negligibly small currents can flow on the nightside, and so the net zonal current on the dayside of the terminator must be negligibly small also. A negative polarization charge therefore develops at the terminator, leading to an eastward zonal field E_ϕ on the dayside and a westward field on the nightside. The resulting $J_{\phi\phi}$ on the dayside just balances $J_{\phi\theta}$, and E_ϕ maps to the F region to produce the observed upward and then downward $\mathbf{E} \times \mathbf{B}$ drift.

This picture does give us some insight, but it is too oversimplified. The timing of the enhancements and reversals is not quite right, and it is not clear what will happen in the E region at the equator, where there is no direct coupling to the F region. A somewhat more complicated, but still reasonably simple model of the interactions is sketched in Figure 8.

This rather complicated figure shows currents within and into/out of the E layer, currents flowing parallel to the magnetic field up into the F region on the bottomside and down out of the region on the topside, and some of the associated electric fields. These parallel coupling currents are just what are shown in Figure 6 and are fairly easily explained. It turns out that the most important contribution to $\nabla_\perp \mathbf{J}$ in the F region at the equator comes from the vertical derivative of the vertical current, and it is straightforward to show that this current is given by

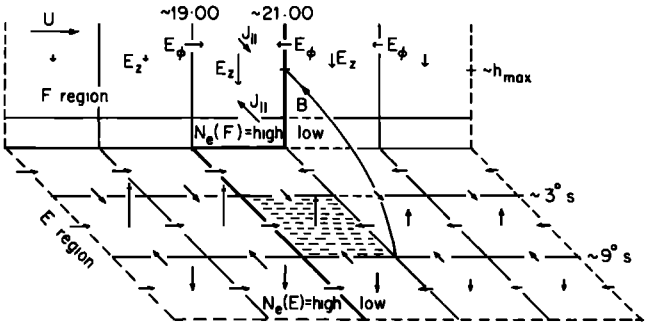

Fig. 8. More realistic model of the prereversal enhancement. The F region wind U forces currents to flow into the bottomside F region and out of the topside, in proportion to the F region electron density. This current remains strong in the early postsunset period, in spite of the low E layer densities, and so E layer currents must flow into the region shown negatively charged. The associated electric fields cause an upward, then downward, F region drift and an eastward, then westward, E region electrojet (westward, then eastward, electron drift). See text for further details.

$$J_z = Ne \frac{\nu_i}{\Omega_i} (U - V_{i\phi}) \tag{2}$$

where U is the eastward wind velocity, ν_i and Ω_i are the ion collision and Larmor frequencies, and $V_{i\phi}$ is the eastward ion drift velocity. Only N and ν_i vary rapidly with height, and so

$$\frac{\partial}{\partial z} J_z \propto \frac{\partial}{\partial z} (N\nu_i) \tag{3}$$

$$J_\parallel \propto \int \frac{\partial}{\partial z} (N\nu_i)\, ds \tag{4}$$

where the integration is along a magnetic field line from the top of the low-latitude E region to the top of the field line at the equator. For our model ionosphere the integration in (4) is positive for field lines that map to the equator in the lower F region and negative for the upper F region, reversing somewhere near h_{max}, which corresponds to an E region latitude in the vicinity of 9°–10°, as is illustrated in Figure 6.

We can visualize the F region as a dynamo which extracts current from two narrow strips of the E region centered at about 6° latitude in each hemisphere and returns it to two broader strips centered at 10°–11°. During the day this generator acts as a constant current source, limited by its internal impedance rather than by the E region load. At sunset, as the E region density drops to its more or less constant nighttime value, the load impedance rises suddenly and becomes comparable to the generator impedance, reducing the current somewhat (via the increase in $V_{i\phi}$) but increasing the E region electric fields substantially. As the night progresses, the F region generator impedance rises slowly as the F layer density decreases, and both the F dynamo currents and fields decrease.

The details of the E region currents and fields are complicated by the fact that the two-dimensional E layer conductivity is anisotropic and a strong function of latitude, as well as time (longitude), in this sunset period. The area most directly associated with the prereversal enhancement consists of the two strips centered about 6° from the equator and extending for 1–2 hours after sunset. The strong upward current which the F region extracts from this region of low conductivity must be pulled in somehow from other parts of the E region. This means that this current sink area must develop a negative polarization charge so that strong electric fields are directed toward it, namely, eastward, then westward, fields at earlier and later times and equatorward fields at higher latitudes. At very low latitudes the meridional field is poleward (see Figures 5 and 6), but it is very small because the north-south conductivity $\Sigma_{\phi\phi}$ is high since the magnetic field is nearly horizontal. A consequence of these small meridional fields is that the zonal fields are nearly independent of latitude below 10° or so, and therefore they also will be approximately the same in the E and F regions at the equator. These characteristics are all completely in accord with the observed prereversal enhancement. There are usually no comparable effects near the sunrise period because the F region/E region conductivity ratio is smaller then than at sunset and the F region dynamo is less important.

This picture will not change in a qualitative way even if the ionospheric model is changed substantially. *Anderson and Mendillo* [1983], for example, calculate that the integrated (along **B**) F region Pedersen conductivity continues to increase with altitude to well above h_{max} because of the effect of the equatorial anomaly, which we have neglected. For such an ionosphere $J_\parallel$, calculated from (4), will not reverse to downward at about 9° latitude, as is shown in Figures 6 and 8, but this change just means that the negatively charged current sink strip in Figure 8 must extend to higher latitudes.

So it seems that this simple model based on a constant eastward F region wind can account for the prereversal enhancement of the electric fields quite adequately. Day-to-day, seasonal, and solar cycle changes in the prereversal enhancement will result from such things as (1) variations in the F region wind, (2) changes in the E/F conductivity (i.e., density) ratio, (3) E region dynamo contributions, which can be comparable to those of the F region, and (4) the effects of the lack of symmetry between the hemispheres and the noncoincidence of the geographic and dip equators [*Walton and Bowhill*, 1979]. During nonequinoctial periods, for example, the different sunset times in the two hemispheres will make the sunset effect less abrupt, and therefore the prereversal enhancement should be less pronounced.

Acknowledgments. We thank D. Anderson for some helpful discussions. This research was supported by the Atmospheric Sciences Division of the National Science Foundation through grants ATM-8218619, ATM-8418717, and ATM-8418473. One of us (E.B.) received fellowship support from the Conselho Nacional de Pesquisa of Brazil. The work was completed while one of us (D.T.F.) was on leave at the Uppsala Ionospheric Observatory and the Kiruna Geophysical Institute in Sweden. The kind hospitality and support of both institutions was much appreciated.

The Editor thanks H. Maeda and H. Rishbeth for their assistance in evaluating this paper.

REFERENCES

Anderson, D. N., and M. Mendillo, Ionospheric conditions affecting the evolution of equatorial plasma depletions, *Geophys. Res. Lett.*, *10*, 541, 1983.

Balsley, B. B., Electric fields in the equatorial ionosphere: A review of techniques and measurements, *J. Atmos. Terr. Phys.*, *35*, 1035, 1973.

Balsley, B. B., and R. F. Woodman, On the control of the F-region drift velocity by the E-region electric field: Experimental evidence, *J. Atmos. Terr. Phys.*, *31*, 865, 1969.

Bonelli, E., Equatorial electric fields: A numerical model, Ph.D. thesis, Cornell Univ., Ithaca, N.Y., 1985.

Fejer, B. G., The equatorial ionospheric electric fields: A review, *J. Atmos. Terr. Phys.*, *43*, 377, 1981.

Fejer, B. G., D. T. Farley, R. F. Woodman, and C. Calderon, Dependence of equatorial *F* region vertical drifts on season and solar cycle, *J. Geophys. Res.*, *84*, 5792, 1979.

Heelis, R. A., P. C. Kendall, R. J. Moffett, D. W. Windle, and H. Rishbeth, Electrical coupling of the *E*- and *F*-regions and its effect on *F*-region drifts and winds, *Planet. Space Sci.*, *22*, 743, 1974.

Jacchia, L. G., Thermospheric temperature, density, and composition: New models, *Spec. Rep. 375*, Smithson. Astrophys. Obs., Cambridge, Mass., 1977.

Matuura, N., Electric fields deduced from the thermosphere model, *J. Geophys. Res.*, *79*, 4679, 1974.

Richmond, A. D., S. Matsushita, and J. D. Tarpley, On the production mechanism of electric currents and fields in the ionosphere, *J. Geophys. Res.*, *81*, 547, 1976.

Rishbeth, H., The *F*-layer dynamo, *Planet. Space Sci.*, *19*, 263, 1971.

Rishbeth, H., The *F*-region dynamo, *J. Atmos. Terr. Phys.*, *43*, 387, 1981.

Stening, R. J., A two-layer ionospheric dynamo calculation, *J. Geophys. Res.*, *86*, 3543, 1981.

Takeda, M., and H. Maeda, *F*-region dynamo in the evening—Interpretation of equatorial ΔD anomaly found by MAGSAT, *J. Atmos. Terr. Phys.*, *45*, 401, 1983.

Tarpley, J. D., The ionospheric wind dynamo, 2, Solar tides, *Planet. Space Sci.*, *18*, 1091, 1970.

Walton, E. K., and S. A. Bowhill, Seasonal variations in the low latitude dynamo current system near sunspot maximum, *J. Atmos. Terr. Phys.*, *41*, 937, 1979.

E. Bonelli, Departmento de Fisica, Universidade Federal do Rio Grande do Norte, 59000 Natal, RN, Brazil.

D. T. Farley and B. G. Fejer, School of Electrical Engineering, Phillips Hall, Cornell University, Ithaca, NY 14853.

M. F. Larsen, Department of Physics and Astronomy, Clemson University, Clemson, SC 29631.

(Received June 18, 1986;
revised August 21, 1986;
accepted July 16, 1986.)